On the optimal level of complexity for the representation of groundwater-dependent wetland systems in land surface models

Mennatullah T. Elrashidy[1], Andrew M. Ireson[1,2], Saman Razavi[1,2]

[1]Department of Civil, Environmental and Geological Engineering, University of Saskatchewan, Saskatoon, Canada
[2]School of Environment and Sustainability, University of Saskatchewan, Saskatoon, Canada

Correspondence to: Mennatullah T. Elrashidy (menna.elrashidy@usask.ca)

Abstract. Wetland systems are among the largest stores of carbon on the planet, the most biologically diverse of all ecosystems, and dominant controls of the hydrologic cycle. However, their representation in Land Surface Models (LSMs), which are the terrestrial lower boundary of Earth System Models (ESMs) that inform climate actions, is limited. Here, we explore different possible parametrizations to represent wetland-groundwater-upland interactions with varying levels of system and computational complexity. We perform a series of numerical experiments informed by field observations from a particular type of wetlands, called fens, at the well-instrumented White Gull Creek in Saskatchewan, in the boreal region of North America. In this study, we focus on how modifying the modelling connection between the upland and the wetland affects the system's outcome. We demonstrate that the typical representation of groundwater-dependent wetlands in LSMs, which ignores interactions with groundwater and uplands, can be inadequate. We show that the optimal level of model complexity depends on the land cover, soil type, and the ultimate modelling purpose, being nowcasting and prediction, scenario analysis, or diagnostic learning.

1 Introduction

The Canadian boreal region covers about half of the land area of Canada. Around 85% of all Canadian wetlands (~ 3 million Km[2]) are located in the boreal region (Mitsch, 1991). Wetlands are vital elements in landscapes as they can mitigate the effect of floods, store carbon from the atmosphere, improve water quality, absorb pollutants, and provide a habitat for a wide range of endangered wildlife and plants (Mitsch et al., 2013). Types of wetlands are bogs, fens, swamps, marshes, and shallow water. Each type of wetlands differs in terms of hydrology, water level, morphology, vegetation, and biological aspects (Canada Committee on Ecological (Biophysical) Land Classification, 1988). Fens are wetlands that have accumulated peat of over 40 cm, hydrologically interact with the surrounding groundwater and surface water, and maintain water level at or above ground level for most of the year (Gingras et al., 2018). Fens constitute around 65% of the peatland area within the boreal plain ecozone (Goodbrand, 2013). Fens critically depend on groundwater discharge fluxes to sustain their moisture and water levels. Understanding the lateral hydrological interactions between groundwater (GW) and surface water (SW) in groundwater-dependent wetland/fen systems is crucial to improve their representation in Land Surface Models (LSMs) (Rivera, 2014). Such

improvements can directly improve the simulation of land's energy and water balance as well as different hydrological cycle components like evaporation and streamflow (Blyth et al., 2021).

LSMs were originally proposed to estimate the vertical fluxes (energy and water) of the land surface, which is a necessary lower boundary condition for climate models (Manabe, 1969). Over the past decades, these models have extensively been

35 modified to represent different processes such as soil moisture and vegetation dynamics. However, many recent studies have highlighted the deficiencies in the current LSMs and discussed the scientific motivation to improve their process representations (Clark et al., 2015; Davison et al., 2016; Fan et al., 2019). Lateral water movement, groundwater dynamics, wetland hydrology, hillslope hydrology, and GW-SW interactions are examples of the elements which are either missing or need more realistic representation. The representation of these processes requires the inclusion of sub-grid heterogeneity in

40 LSMs (Blyth et al. 2021). Capturing the complex interactions and heterogeneity of fine-scale landscape features, would enable LSMs to provide more realistic and reliable simulations, facilitating a better understanding of land-atmosphere interactions and their implications for climate dynamics (Fan et al. 2019).

Significant advancements have recently been achieved in representing both vertical and lateral water exchange of GW with surface water in LSMs (de Graaf et al., 2017; Fan et al., 2013; Maxwell et al., 2015); however, most of these efforts have

45 focused one-way process coupling (i.e., water moves in one direction from surface water to GW as recharge), and any feedback from the GW system to the surface water system has been neglected. Multiple studies have implemented two-way coupling between the GW aquifer and soil column within LSMs such as VIC and CLM) to enhance GW system simulation (Scheidegger et al. 2021; Zampieri et al. 2012; Zeng et al. 2018). Zampieri et al. (2012) introduced a simple parametrization in CLM v3.5, which allowed for river-GW bi-directional flow. This parametrization showed an improvement in the soil moisture and surface

50 temperature simulations. Zeng et al. (2018) developed a module for simulating lateral water exchange between grid cells, integrating it into CLM4.5. This module facilitates lateral exchange between grid cells but does not allow lateral exchange between groundwater and rivers. Scheidegger et al. (2021) incorporated a groundwater model in the VIC model that allows for a bi-directional water exchange between the soil and GW aquifer. Their study showed that including the 2D groundwater model significantly affected evapotranspiration, runoff, and recharge of the different simulated grid cells (computational

55 elements). Despite these recent efforts, a significant research gap remains in effectively representing the two-way lateral exchange between groundwater and open water bodies, including lakes and wetlands.

Typically, the coupling between different processes can be represented through one of three approaches: uncoupled, one-way coupled, or two-way coupled. The choice of the appropriate approach depends on the desired complexity level that can predict the variables of interest (Ogden, 2021). The literature generally demonstrates that coupling different models can improve the

60 simulation of various hydrological cycle components including runoff, soil moisture, and water table fluctuations. However, such 'full' coupling approaches can be both systematically and computationally complex, often rendering their applications impractical. In addition, constraints in data availability, especially concerning sub-surface processes, can limit the applicability of complex approaches. Therefore, in practice, more parsimonious approaches to accounting for SW-GW interactions may be 'optimal' for specific modelling goals (Blyth et al., 2021; Ogden, 2021). What has remained elusive, however, is a thorough

65 characterization of tradeoffs between model complexity and adequacy to represent SW-GW processes for a particular landscape and variables of interest (Yalew et al., 2018). Another factor that affects the selection of optimal model complexity is the ultimate modelling purpose. Models can be used for 1) nowcasting and prediction, which focuses on simulating and predicting the expected behaviour of the system of interest in the near future, 2) scenario analysis, wherein the model simulates the system under long-term changing conditions, and 3) diagnostic learning, which focuses on understanding how the system

70 behaved during a historic period (Razavi et al., 2022). Ultimately, the selection of optimal model complexity will depend on the specific modelling task, the available data, and the desired level of accuracy.

Here, to address this gap, we aim to characterize the optimal level of complexity required to represent the interactions between uplands, groundwater, and wetlands in different landscape configurations. To achieve this, we conduct a series of modelling experiments using four approaches, ranging from a full disconnect to full coupling. We particularly focus on a well-

75 instrumented and studied fen system in the Boreal region of North America. Our primary objective is to examine how the simulated upland and fen systems respond to changes in modelling complexity. The GWT observations are utilized to derive a reasonable set of parameters representing the upland-GW-fen system. Additionally, through numerical experiments, we investigate the performance of surface water fed wetland, providing a contrasting non-fen wetland scenario against the groundwater-dominated case. Based on insights gained in these experiments, we provide some recommendations on how to

80 improve LSMs in representing critical processes related to wetland types such as fens – processes that are often missing or poorly represented in the current generation of LSMs.

2 Study Area and Data

The study area is located within the White Gull Creek basin (WGCB), located north of Prince Albert, Saskatchewan (Barr et al., 2012), shown in Figure 1. The study area and transect are set using the Canadian Digital Elevation Model (CDEM,

85 (Canadian Digital Elevation Model, 1945-2011 - Open Government Portal, 2022)).
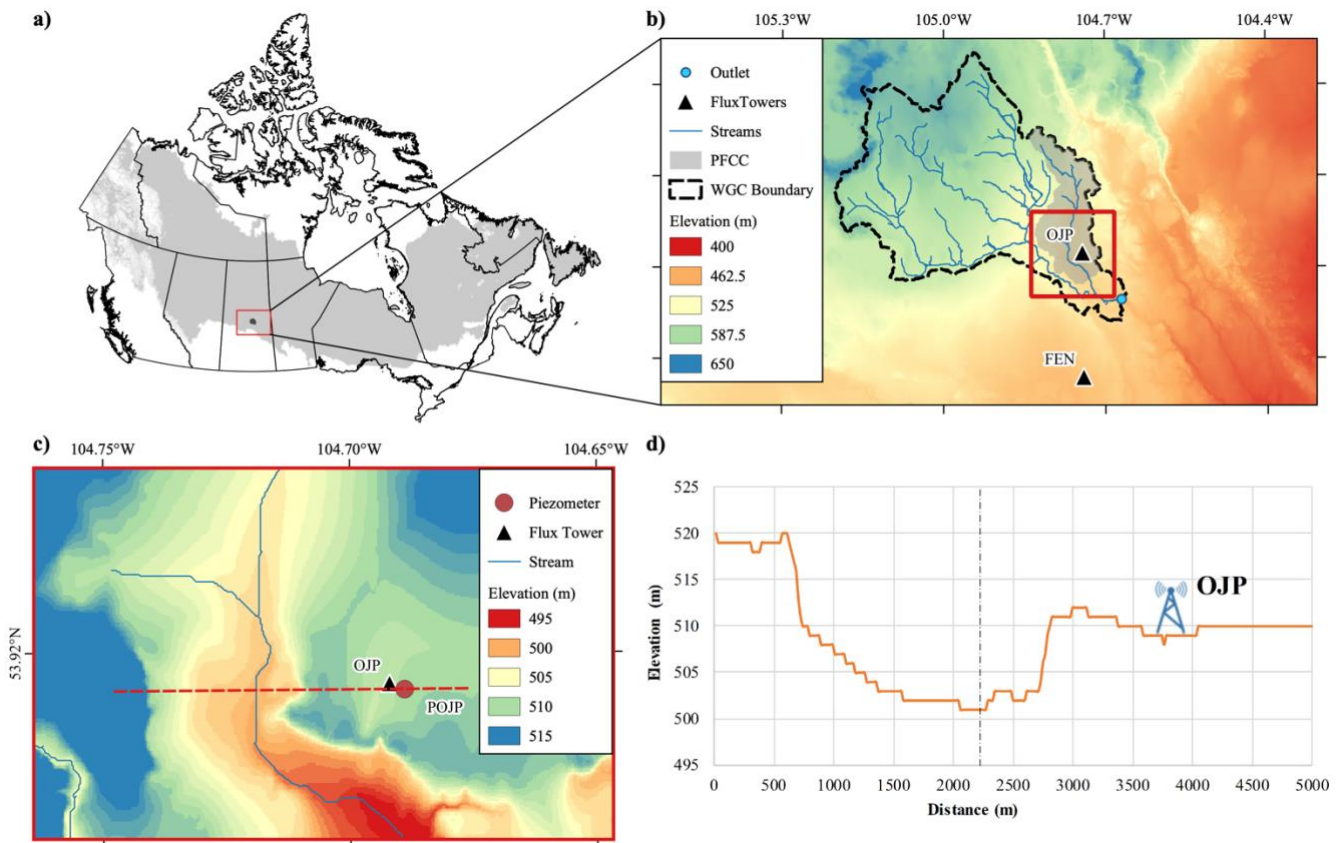
Figure 1: Detailed view of the study area. a) Canada's boreal region in a gray shade, b) A focused view of the White Gull Creek basin (WGCB) area and the two flux towers used in the study (Old Jack Pine (OJP) and Fen). The shaded gray area represents the Pine Fen Creek Catchment (PFCC) that include the Pine Fen (PF), c) Focused view on OJP area, the Piezometer of OJP (POJP), and the Pine Fen (PF), d) Cross-section of OJP and the PF (the dashed black line is assumed to be the line of symmetry).

The upland is the area around the Old Jack Pine (OJP) flux tower (Latitude 53.92° N and Longitude 104.69° W) (Figure 1), which is part of the Boreal Ecosystem Research and Monitoring Sites (BERMS). The upland transect ends at the boundaries of WGCB, and the OJP site is located roughly in the middle of the transect (Figure 1-d), and is collocated with the piezometer (POJP, Figure 1-c) that is used to calibrate and validate the model performance. The transect length of 3450 m is divided into the upland hillslope, 3300 m in length, and the 150 m wide fen (which is half the total width of the fen). At the OJP site, the dominant land cover is Jack pine (Pinus banksiana Lamb), and the soil is sandy textured, which has poor nutrition and high drainage with a water table around 5m below ground (Barr et al., 2012). The meteorological data at OJP are available each 30 min for 23 years from 1997 to 2018. The groundwater table (GWT) observations are available at POJP location (Figure 1) from 2003 to 2018.

The lowland part of our transect is a fen known as Pine Fen (PF) which is situated in Pine Fen Creek catchment (PFCC), a tributary of WGC (39.9% of PFCC land cover is peatland) (Goodbrand et al., 2019). The PF site is a peatland mosaic

surrounded by forests of jack pine and black spruce. The average peat thickness is 0.65m with a maximum depth of about 2m. Unfortunately, we do not have direct meteorological observations from PF, and therefore as a proxy for this we use observations from the BERMS fen flux tower site (FEN hereafter). FEN is located just outside WGCB boundary, about 8 km south of the basin (Latitude 53.78° N and Longitude 104.69° W) (Figure 1-b). The FEN and PF sites are similar in terms of the peat-soils, vegetation, and topography, so the FEN is considered a reasonable proxy for the vertical fluxes at the PF. At the FEN, forcing data are recorded with a 30-minute resolution from 2003 to 2018, and the observed evapotranspiration rates (ET) are from 2004 to 2010 and from 2013 to 2019 at 30 min intervals.

3 Upland-Groundwater-Fen Model Description

3.1 Conceptual Background

Our study is based on a real field site, using real field observations, as described in the previous section. However, this site is not a perfectly constrained hillslope-fen system, i.e., a hillslope with 1D horizontal flow and a no-flow boundary condition at the interfluve. Therefore, we use an abstracted hypothetical hillslope configuration to simulate the vertical and lateral flows of water between atmosphere-upland-groundwater-fen system. This configuration is physically realistic, allowing us to test the implications of different hillslope-fen coupling mechanisms in a controlled manner Figure 2.

Our model has three distinct components: (1) the upland soil water balance, which generates groundwater recharge and runoff; (2) a lateral groundwater flow model beneath the upland, that may discharge water into the fen; and (3) a simple fen water balance model, that receives inputs from rainfall, snowmelt, runoff and lateral groundwater discharge (in some cases), and loses water to evaporation and discharge into a stream channel.

The model is driven by site observations of precipitation and other meteorological variables. A typical LSM is used to simulate evapotranspiration fluxes in the upland and fen, groundwater recharge, runoff fluxes from the upland, and snowmelt into the fen. In this case, runoff fluxes are much smaller compared to the groundwater recharge. The water table and groundwater discharge are simulated by a simple 1D unconfined aquifer model. The water level at the fen and its discharge flux into an adjacent stream are simulated by a simple fen water balance model. The connections between the three models of upland, groundwater and fen are configured in four ways as shown in Figure 2, resulting in four different collective models as follows:

- V0) Uncoupled upland-fen model: The upland soil water balance and the fen are simulated as independent of one another, and there is no groundwater model. Discharge from the upland in the form of surface runoff and soil drainage (baseflow) are combined with the fen discharge and routed into the river. This configuration is representative of many LSMs.

- V1) Uncoupled upland-groundwater-fen model: Soil drainage from the upland recharges the unconfined aquifer. Surface runoff from the upland, groundwater discharge and fen discharge are combined and routed into the river. The upland and the fen are again completely independent of one another. This configuration is representative of an LSM

that has a groundwater store with one-way vertical connection with soil column such as Community Land Model (CLM) and Variable Infiltration Capacity (VIC) models (Clark et al., 2015).

135
- V2) Chained model: Soil drainage from the upland recharges the unconfined aquifer and groundwater discharge contributes to storage into the fen. Discharge from the fen is routed into the river. The groundwater is independent of the fen, but the fen depends on discharge from the groundwater.

- V3) Coupled model: Soil drainage from the upland recharges the unconfined aquifer. Groundwater discharge into the fen is determined based on head gradient between the groundwater and fen, and two-way water exchange is
140
considered between the groundwater and fen. Surface runoff from the upland also goes into the fen. Discharge from the fen is routed into the river. The groundwater and fen are mutually dependent on one another.
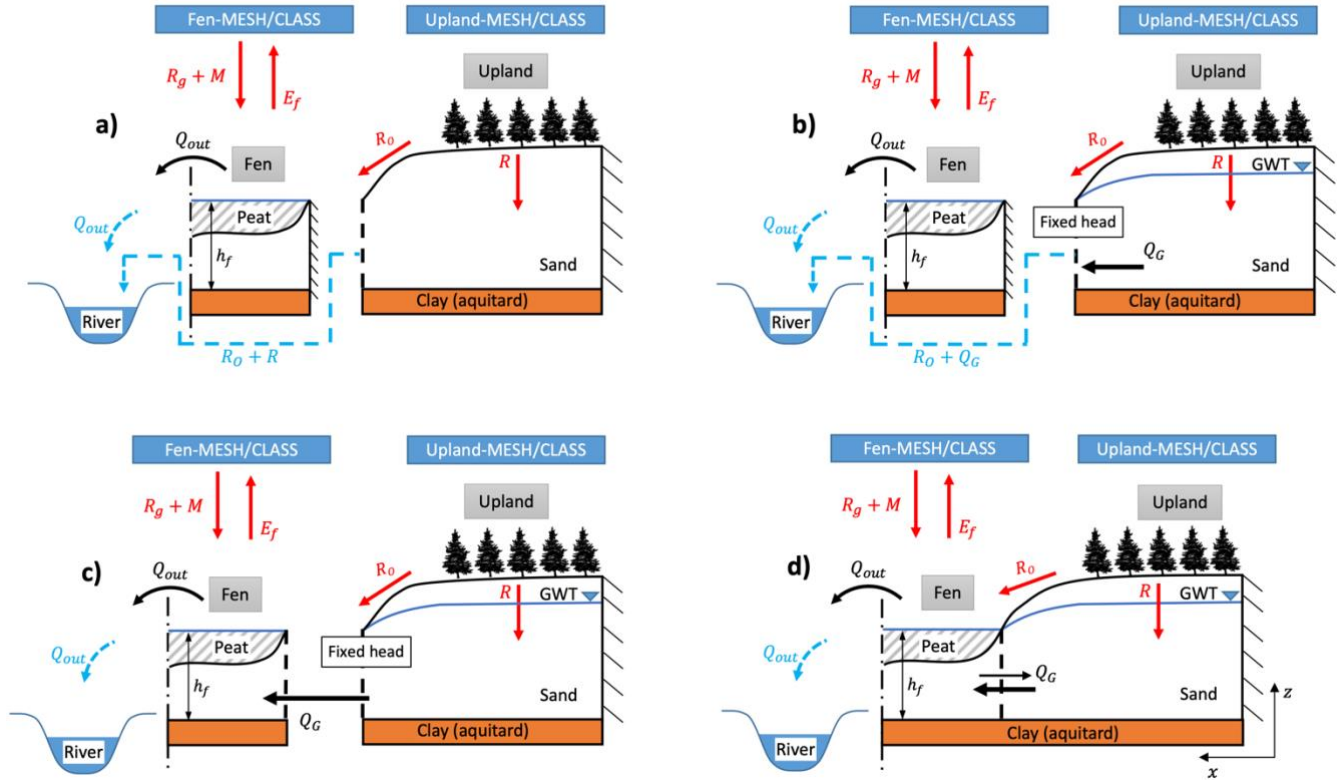
Figure 2: Schematic of the different scenarios of representing the connection between the upland, GW, and fen. a) Uncoupled upland-fen and no GW (V0), b) Uncoupled upland-GW-fen (V1), c) Chained model (V2), d) Coupled model (V3). The vertical fluxes are rain on the ground (R_g), snowmelt (M), Evapotranspiration from the fen (E_f), and soil drainage as recharge into groundwater (R). The lateral fluxes are upland runoff (R_O), and groundwater discharge (Q_G).

3.2 Upland Soil Water Balance Model

The upland soil water balance is simulated using the MESH-CLASS land surface model (Canadian Land-surface scheme; (Pietroniro et al., 2007; Wheater et al., 2022)) in a point-scale setup using the data from OJP site, which is referred to as MESH_OJP. The land cover of the grid cell is represented by one canopy type which is evergreen needle leaf, as most of the vegetation in the OJP area is jack pine trees. MESH_OJP is forced using seven metrological components (precipitation, shortwave radiation, long-wave radiation, wind speed, specific humidity, temperature, and atmospheric pressure), which are collected from the OJP flux tower from 1997 to 2018 every 30 minutes. The soil depth is assumed to equal 4.1 m and is divided into three layers (i.e., the default CLASS configuration). We are mainly interested in two outputs from the model: Soil drainage (R) is used as either baseflow to the river (V0) or recharge to the groundwater (V1-V3); and surface runoff (R_o) is used as surface water input to river (V0, V1) or input to the fen (V2, V3). The MESH-CLASS model uses an infiltration excess based

on Green and Ampt equation to calculate the soil infiltration and the excess ponded water on the top of soil column is used to calculate the overland runoff.

3.3 Upland-Groundwater Model

The groundwater underneath the upland zone is represented as a 1-D horizontal unconfined aquifer, bound by a no-flow boundary on the right (the groundwater divide) and the fen on the left (Figure 2). The problem is governed by 1-D Boussinesq equation:

$$S_y \frac{\partial h}{\partial t} = \frac{K}{2} \frac{\partial^2 h^2}{\partial x^2} + R \,,$$
(1)

Where, S_y (unitless) is the specific yield, h (m) is the head in the aquifer (water table level), t (days) is time, K (m/day) is the lateral hydraulic conductivity, and R (m/day) is the recharge rate.

Equation 1 is solved numerically using a block-cantered finite difference solution on a regularly spaced grid ($dx = 0.01 * L$), integrated in time using the method of lines with the SciPy-ODE solver "odeint" (Virtanen et al., 2020), and the solution is coded up in python. The lateral fluxes are calculated at cell boundaries using Darcy's Law. The initial condition is assumed to be a uniform hydraulic head in the aquifer at the same water level as in the fen (h_f). The right-hand boundary condition is considered as a groundwater divide, and thus, a no-flow condition ($q(x = 0, 0 <= t <= t_{max}) = 0$). The flux on the left-hand boundary is determined using either a fixed head boundary (V1, V2) or based on the head gradient between the groundwater and the fen (V3). The groundwater model is driven by the recharge fluxes (R), which are output from the upland soil water balance model and are assumed to be spatially uniform.

3.4 Fen Water Balance Model

The fen is modelled as a simple lumped store, with the water balance equation.

$$n_f w_f \frac{\partial h_f}{\partial t} = (R_g + M - E_f)w_f + R_O \, L + Q_G + Q_{in} - Q_{out} \,,$$
(2)

Where, n_f (unitless) is the porosity of the fen's material, w_f (m) is the width of the fen, h_f (m) is the water level of the fen, L (m) is the aquifer/hillslope length (in x direction), $R_g, M, E_f,$ and R_O (m/day) are the rainfall, snowmelt, evaporation, and runoff from the upland, respectively, Q_G (m²/day) is the lateral groundwater inflow, and Q_{out} (m²/day) is the outflow from the fen, assuming a unit area of 1m in y direction.

For $E_f, R_G,$ and M, these fluxes are simulated by a point-scale MESH model using the data from the FEN site (MESH_FEN), which reasonably represent the conditions at the PF site. The forcing data (2003 to 2018) from the FEN flux tower are used to drive the MESH-FEN model. To simulate the peatland in the MESH/CLASS model, the land cover is assumed to be grass and the soil type is set to organic soil with three soil layers of changing properties as fibric, hemic, and sapric (Letts et al., 2000).

We manually calibrate the minimum stomatal resistance ($r_{s,min} = 100$ s/m), using local observations of the driving meteorological variables. We compare the simulated E_f with both the observed fluxes and with potential evaporation calculated using the Penman Monteith equation, and we found that all three are consistent, showing that the evaporation from the FEN is unstressed (i.e., not water-limited). The values of Q_G are either zero (V0, V1) or equal to the groundwater discharge at the right-hand boundary (V2, V3).

The values of Q_{out} are generated when a spilling threshold, denoted as h_{spill}, is exceeded. Q_{out} is assumed to be a non-linear function of storage above h_{spill} as given by:

$$Q_{out} = w_f \, c_{spill}(h_{spill} - h_f)^n \tag{3}$$

The value of h_{spill} is assumed to equal the elevation of the fixed head boundary at the uncoupled groundwater model (Figure 2-b/c). The values of c_{spill} and n (coefficient and exponent, respectively) are calibration parameters and are somewhat arbitrarily chosen within reasonable ranges. As there are no available outflow observations at the FEN site to allow for calibration, we adopt the recommended ranges provided by Razavi and Gupta (2019) for a fast reservoir with non-linear response (similar function/response to the fen storage). Razavi and Gupta (2019)'s values of k and *alpha* (coefficient and exponent, respectively) are utilized to define c_{spill} and n values ($c_{spill} = 0.1$ and $n = 1.5$). While this approach lacks specific calibration for our site, it is deemed acceptable for achieving our study's objective, which is to compare different model configurations (V0, V1, V2, and V3) using the same parameters.

4 Model Analysis and Performance Evaluation

4.1 Calibration strategy

The performance of the different collective models is evaluated using the GWT observations at the POJP location by calculating the root mean squared error (RMSE)). For the upland water balance model, we use the same calibrated parameters from the study of (Nazarbakhsh et al., 2020), in which they use the CLASS model to assess the controls of evapotranspiration in the seasonally frozen forest. For the other parameters, Monte-Carlo simulations with 15,000 realizations (randomly generated parameters from a uniform distribution bounded by the feasible parameter space in Table 1) are used to run the uncoupled upland-GW (V1). The behavioural runs are identified as the realizations with RMSE <0.08m (threshold is chosen arbitrarily based on expert judgement and calculated for the period from 2003 to 2009) and are used to perform the uncertainty analysis of GWT simulation. The parameter set with lowest RMSE is considered the calibrated parameter set and is used to validate the model. This parameter set is also used to run all the other collective models throughout the study.

Table 1: Monte-Carlo analysis parameters ranges of the uncoupled upland model.

Parameters	Description	Lower bound	Upper bound	Calibrated parameters
$log(K)(m/d)$	Hydraulic conductivity Logarithm	-1	3	2.13
S_y	Specific yield	0.1	0.5	0.24
$h_f(m)$	Fen's water head	5	20	9
$L(m)$	Hillslope length	3000	3500	3275
$x(m)$	Piezometer location	1700	1800	1733

4.2 Effect of different upland properties

215   We develop two hypothetical numerical experiments to explore the conditions under which different levels of model complexity may be necessary. Experiment 1 focuses on hillslope geometry, by considering five different values of the hillslope length (L, that is the length of the upland). L values of 100, 300, 500, 1000, 2000, and 3000 m are considered, and all other parameters are the same as in the original model setup. This experiment uses the chained (V2) and the coupled (V3) versions of the model. Experiment 2 focuses on soil properties, by comparing the original (sandy soil) setup with a fine-grained soil

220   representative of mineral soil which typically can be found in the prairies area. This is achieved using an alternative configuration of the MESH model, in which the parameters are changed with values to represent a grassland cover and a fine-grained soil texture (clayey soil) resulting in different amounts of runoff, infiltration and soil drainage. In the upland algorithm, the values of K and S_y are set to 1.35m/d and 0.1, respectively, to characterize the fine-grained soil. The simulated GWT and GW fluxes using the new MESH/CLASS run (representing fine-grained soil) are compared with the model results when using

225   the original study setup (upland algorithm forced with MESH-OJP).

5 Results and Discussion

We assess the performance of the model in the upland (Section 5.1) and fen (Section 5.2) independently. Next in Section 5.3, we assess the sensitivity of the simulated outflow from the integrated upland-groundwater-fen system, which corresponds to the outflow on a grid cell scale in LSMs (i.e., the bulk system outflow) to the different model configurations. Lastly, in Section

230   5.4, we describe the results of the two numerical experiments exploring the effect of changed upland properties and different wetland functionality.

5.1 Model performance in the upland

In the upland, the performance of the vertical land surface fluxes is explored by (Nazarbakhsh et al., 2020). We are able to assess the upland model's performance in reproducing observations of the water table elevation. As explained earlier, there is
235 no groundwater in V0 of the model. In the uncoupled (V1) and chained (V2) models, the groundwater simulations are identical. In the coupled model (V3) the water table simulations may, in principle, differ from those in V1 and V2. Therefore, here we compare V1 and V3 separately.

5.1.1 Uncoupled model calibration and validation

The upland component in the uncoupled model is driven by the recharge values that are generated using the MESH-OJP model
240 (Figure 3-a). Figure 3-b shows a comparison between the simulated and observed GWT at OJP site using the uncoupled upland model. The behavioural runs (69 runs with RMSE<0.08m) from Monte-Carlo analysis are used to generate the uncertainty bounds in the simulation of both GW discharge and GWT (Figure 3). It can be seen from Figure 3-a that the recharge and the simulated GW discharge responded to each other consistently. Also, the changes in the GWT corresponded to both the recharge and the GW discharge peaks.
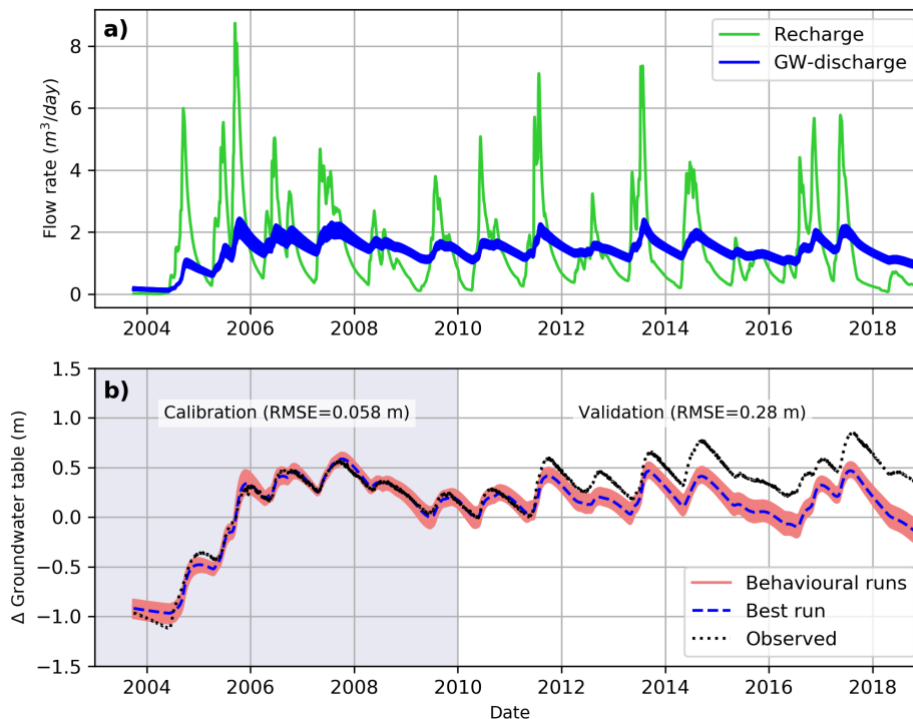
245

Figure 3: a) Upland recharge rates into the groundwater aquifer that are generated using MESH-OJP model and are used to drive the upland component, b) comparison between the simulated (V1) and observed changes in the GWT at OJP site. The uncertainty results (GW discharge and GWT) are obtained from the behavioural realizations using Monte-Carlo analysis.

For the uncoupled upland model, the best value of RMSE is equal to 0.058 m for calibration, and the value for the validation is 0.28 m. The uncoupled upland model can simulate the GWT in the calibration period with a narrow uncertainty bound. In the validation period, the simulated GWT matched the observations until the spring of 2011, when a discrepancy is noticed, and the GWT is underestimated thereafter. The GWT underestimation is caused by low recharge rates from 2011 to the end of the simulation, which might be caused by either undercatch in the observed precipitation or problems with the MESH/CLASS model in simulating the recharge rates at this period. The MESH/CLASS model problem could be because of overestimation of evapotranspiration rates at the upland site, which means the MESH/CLASS model might need re-calibration to a longer period of data. We should note that although the model showed underestimation of the GWT magnitude (from 2011 to 2018), it captured the same pattern during the same period. We believe that our model performance acceptably serves the purpose, as the main purpose of this study is to perform numerical experiments to help us understand the upland-groundwater-fen system dynamics.

5.1.2 Upland-Uncoupled vs Coupled

Figure 4 shows a comparison between the simulated GWT using the uncoupled/chained (V1/V2) and coupled (V3) model versions, and the observations (the uncoupled upland (V1) has the same function in the case of chained model (V2)). The overall performance of the coupled version showed only a slight improvement (RMSE=0.18m) over the uncoupled version (RMSE=0.22m). A comparison between the simulated uncoupled and coupled systems shows that, in the period of record, considering the effect of the fen system does not affect the simulated GWT underneath the upland in the case of OJP and PF. However, the impact of this coupling might become more profound for other sites with different settings or the same site under different climate conditions.
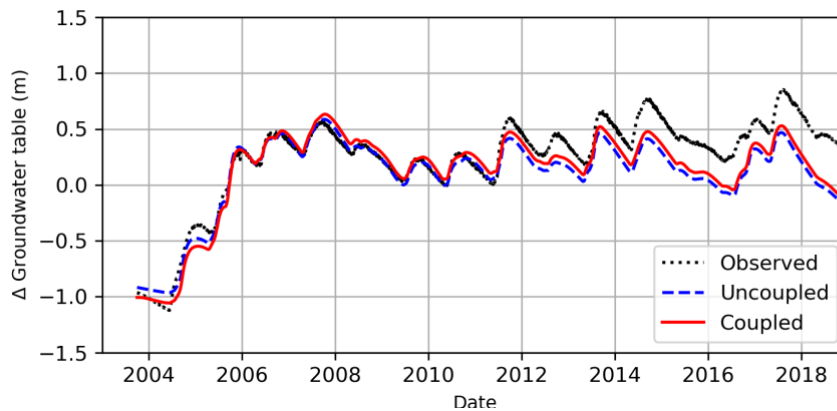
Figure 4: Comparison between the simulated GWT using both the uncoupled and coupled models with the observations.

 5.2 Model performance in the fen

For the fen, we are not able to directly test our model performance due to a lack of data, and instead, we explore the sensitivity of the fluxes to the change in the modelling configuration (interaction between the upland and fen). The fen's outflow and changes in water level are compared for the three versions (V1, V2, and V3) in Figure 5. In the uncoupled (V1) model, when there is no groundwater inflow to the fen, the estimated outflow and water level changes are unrealistic as the outflow is almost

275 zero and the water level kept decreasing from one year to another. On the other hand, the chained (V2) and coupled (V3) models had a reasonable simulation of the outflow and water level changes of the fen but with differences from each other particularly in terms of flow rate. The overall trends of flow rates of V2 and V3 look similar, but the higher-frequency features (e.g., daily flows) show different dynamics from time to time. Flow rates of V3 are affected by the two-way water exchange between the upland and fen, which are based on the variable fen water level, unlike the concept of constant fen water level that

280 is used in V2. This is apparent in 2004, wherein V3 model generated negative flow rates (i.e., water flows from the fen into the upland). This comparison shows that the groundwater inflow from the upland into the fen cannot be ignored when simulating the fen, however, the chained modelling approach might be deemed adequate to capture the fen system dynamics. Coupled configuration is needed to study the short-term impacts and changes in the fen outflow.
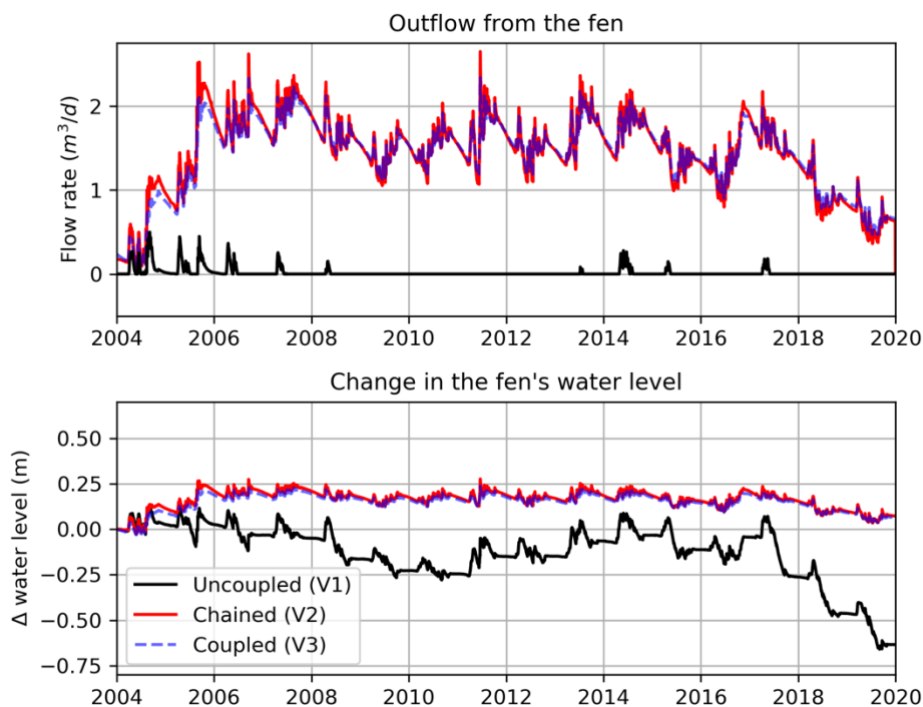
285 **Figure 5: Comparison between the fen's output (fen outflow and change in the fen water level) for the three modelling scenarios (uncoupled (V1), chained (V2), and coupled (V3)).**

5.3 Outflow of The Integrated Upland-Fen System (Grid-cell scale)

In this section, we investigated the total outflow from the integrated upland-GW-fen system as a whole unit under different modelling configurations, which are the possible approaches to represent such system in LSMs, to simulate the amount of the total flow that discharges into the river network (streamflow) (check blue dotted arrows in Figure 2). In LSMs, a grid cell can contain multiple components, such as upland and fen. In this case, the total outflow of the grid cell is the combined outflow from both the upland and fen components after considering the interaction between them based on the used modelling configuration. This is done to assess the optimal level of model complexity that can simulate the streamflow adequately.

In the chained (V2) and coupled (V3) models, the simulated GW discharge into the fen from both models are almost the same at a daily and annual scale (Figure 6). Also, the total outflow from the grid cell into river had no significant difference in the two cases. In the case of uncoupled upland-GW and fen model (V1), there is no GW discharge into the fen, but the daily and annual total outflow into the river is similar to that of V2 and V3. Therefore, on the grid cell scale, the interaction between upland and the fen had no effect on the total outflow from the grid cell and discharge into the river for our model configuration. In case of V0, when there is no account for the GW storage and all the soil drainage (recharge) is considered as baseflow, which is discharged directly into the river network (the case in most of the current LSMs). Therefore, the simulated outflow (of V0) into the river is significantly different (with overall greater magnitudes) compared to the other three versions that accounts for GW storage (Figure 6). That means considering the GW dynamics underneath the upland is essential for a reasonable simulation of the total streamflow into the river network.
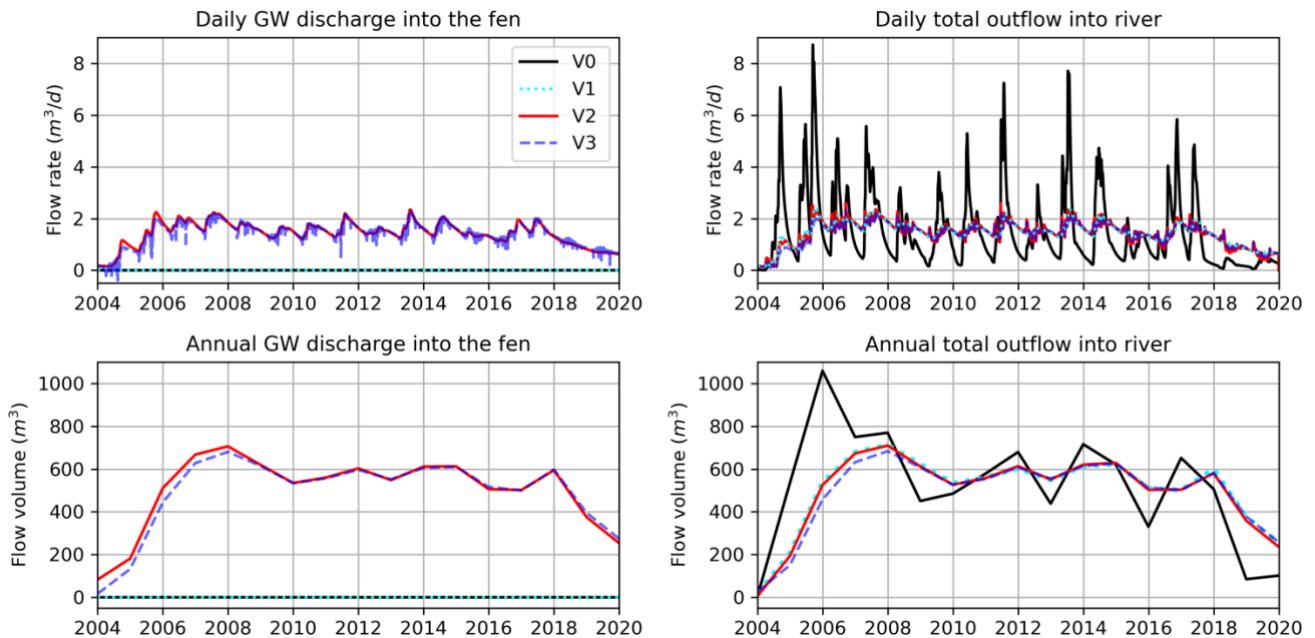
305 **Figure 6: Comparison between GW discharge into fen and total outflow form grid cell into river on daily and annual scales for V0, V1, V2, and V3 modelling scenarios (Figure 2)**

5.4 The effect of different upland properties on the upland-fen interactions

Here, we run two additional numerical experiments to explore the optimal level of modelling complexity for different upland site properties. The experiments are hypothetical (no observations) and represent other possible sites' conditions.

5.4.1 Experiment 1: Different hillslope lengths

Figure 7 shows the simulated upland GWT using different upland hillslope lengths (width of the fen is constant) and compares the results in the case of chained (V2) and coupled (V3) upland. In the case of horizontally large aquifers ($L > 1000m$), as in our original study setup, there is no significant difference in the simulated GWT and GW flux when using the two model configurations. In contrast, in small hillslopes (lengths between 100 to 500 m), the chained model is not able to reasonably
315 capture the fluctuations of the upland GWT (GWT is almost constant), due to a fixed head boundary condition at the upland side. Also, the difference can be seen when comparing the simulated GW fluxes in the two model configurations (Figure 8). In small hillslopes, the coupled model can capture the water amounts that move from the fen into the upland (negative flux values), which are considerable amounts frequently present throughout the year.
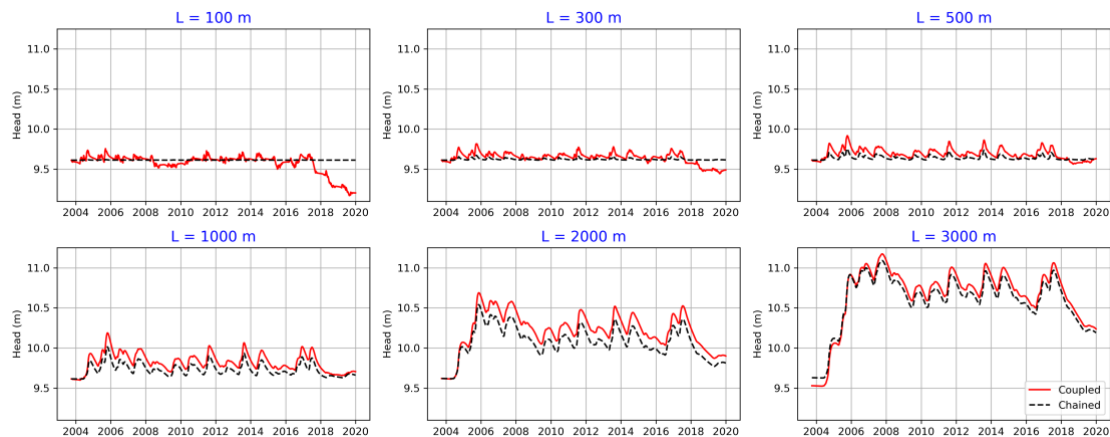
320 **Figure 7: Simulated upland GWT for both Chained and coupled model versions by using different hillslope length (L).**
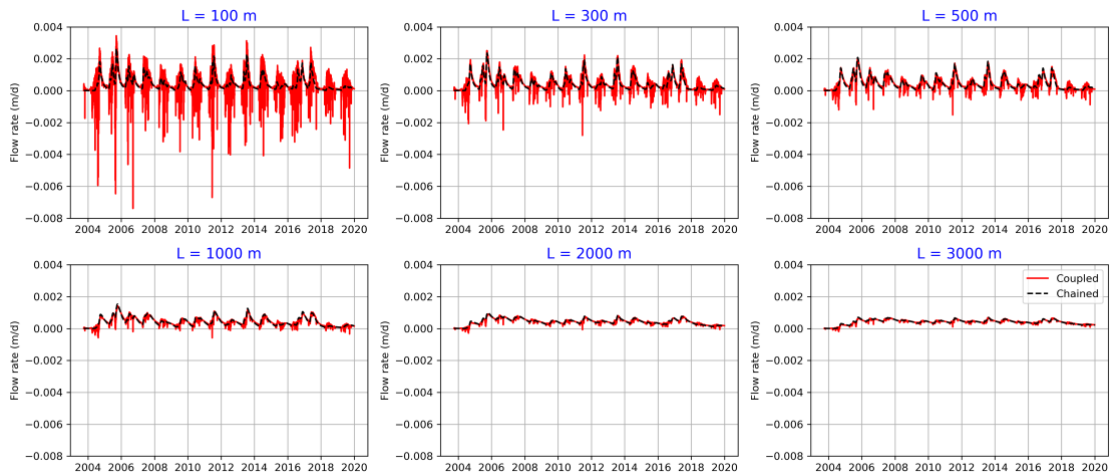
Figure 8: Simulated upland GW fluxes for both chained and coupled model versions by using different hillslope length (*L*).

In the case of large hillslopes, the groundwater size is significantly greater than the fen size (140m) and therefore large amounts of water move from the upland into the fen. As a result, the upland controls the dynamics of the whole system. In such cases, the upland can be simulated independently with no account for the interaction with the fen. In the case of small hillslopes, however, the fen is the dominant contributor to the system as the water moves continually in two-way directions. In such cases, the coupling between the upland and fen is essential.

5.4.2 Experiment 2: Different upland soil properties

Figure 9 illustrates a comparison between two upland cases: 1) coarse-grained soil (high permeability) and forest land cover (dense vegetation) with a long hillslope length, which is our original study setup (Figure 9-a); and 2) fine-grained soil (low permeability) and grass land cover (Figure 9-b). In MESH_OJP, changing the vegetation type impacts evapotranspiration rates from the upland and R_O, while altering the soil properties affects the infiltrated water and R rates. In this experiment, the first case represents the original model configuration at OJP, while the second case is designed to maximize surface runoff from the upland into the wetland. This provides a contrasting scenario with a different wetland type other that fens, in contrast to the groundwater-dependent wetland case. The parameters used to configure the MESH model for the second case are based on a model configuration presented in Ireson et al. (2022) and are similar to the parameters and properties of the St. Denis site. In the case of coarse-grained soil (Figure 9-a), the main contribution to the upland GW system is the high recharge rates because of the high infiltrability of the soil (coarse-grained/sandy), and relatively very small amounts of surface runoff to the fen. Thus, in this case, the dominant component of the upland-fen system is the GW water fluxes from the upland into the fen (through the subsurface water movement). Water arrives as precipitation on the upland, infiltrates into the soil and recharges the aquifer, and finally moves laterally in the aquifer to discharge into the fen. To represent these system dynamics, the chained (V2) modelling approach for the upland system seems adequate to simulate the GW system (GWT and GW discharge) of the

upland (this might not be applicable to relatively small hillslopes, as demonstrated in Experiment 1 (Section 5.4.1)), as the difference between the results when using chained (V2) and coupled (V3) models is relatively small (Figure 9-a). However, the coupled (V3) model can simulate the dynamics of the daily GW flows due to the frequent change of the fen water level. Accordingly, the flow direction is reversed to be from the fen into the upland (negative flow values) from 2004 to 2005 (Figure 9-a).
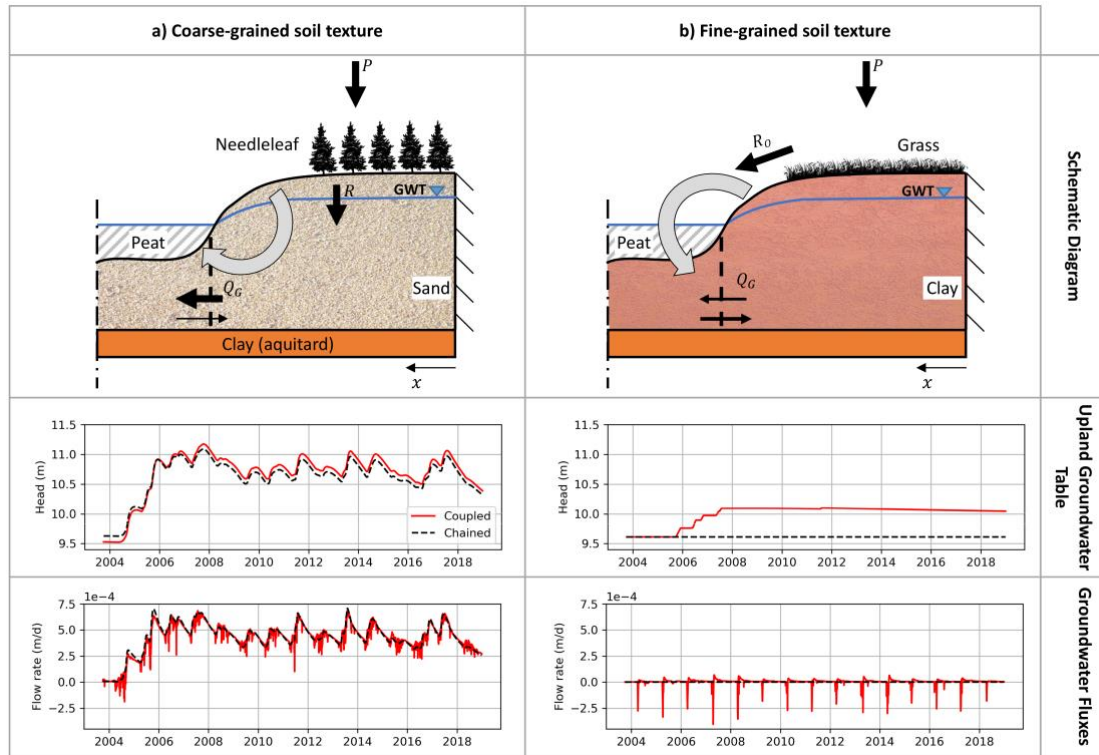
Figure 9: Comparison between two different upland site conditions and simulated upland GWT at each case, a) OJP with coarse-grained soil texture and evergreen needleleaf canopy, b) St Denis with fine-grained soil texture and grass land cover.

The systems dynamics are different when the soil has fine-grained texture, and the vegetation has low density (Figure 9-b). In this case, large amounts of surface runoff move directly from hillslope into the wetland whereas very limited water may infiltrate into the upland aquifer. Figure 9-b shows that the chained model is not able to simulate any of the GW dynamics underneath the upland, whereas the coupled model captured the system's dynamics (Figure 9-b-GW Fluxes). The wetland in this case is mainly fed by the surface runoff fluxes, then the water moves laterally into the upland (especially during snowmelt season). Hence, the main flow path is from the wetland into the upland GW. That means, the upland GW dynamics are dominated by the subsurface water fluxes coming from the neighbouring wetlands. It is obvious that considering only the chained approach (one-way exchange between upland and wetland) in the case of fine-grained upland soil cannot reasonably

capture the real dynamics of the system. However, the full coupling between the upland and the wetland (two-way water

360   exchange) allows the model to represent the actual dynamics of the upland aquifer underneath fine-grained soil layers.

6   Conclusions

The insights gained from applying alternative model configurations to the upland-fen system in this study are as follows:

1.   We were able to reasonably simulate the GW dynamics underneath the upland using the 1D Boussinesq equation. There are no significant differences between the coupled and uncoupled modelling approaches for simulating the

365   upland water table elevation because the dominant flow direction is from the upland to the fen.

2.   To accurately simulate the water level in the fen, it is important not to ignore the GW input from the upland. However, there is no significant difference between the chained (one-way interaction) and coupled (two-way interaction) approaches in terms of the simulated fen water level and outflow.

3.   Including upland-fen interactions had no significant impact on the discharge into the river network. However, the

370   inclusion of GW storage had a major impact on the timing and magnitude of river discharge.

We found that when the size of the fen is large relative to the upland, using a coupled fen-upland modelling approach becomes essential. This is due to substantial bi-directional water exchanges between the fen and the upland GW at various times of the year. The coupled modelling approach is also more likely to be necessary when simulating uplands with fine-grained soils. In this case, the wetland receives more surface runoff and less groundwater input, resulting in a significant loss of water to the

375   groundwater system.

In general, if the main objective of the model is to simulate streamflow, the coupling (two-way interaction) between the upland and fen (or groundwater-dependent wetland types) can likely be ignored. However, groundwater dynamics must be represented in LSMs as they significantly affect the total outflow (streamflow) from the entire system. Conversely, if the simulation of the storage and fluxes within fen/wetlands are of interest, the chained modelling approach represent the least complex level

380   necessary to account for the contributions of the surrounding upland and GW systems.

This study provides insights into the necessary model complexity for simulating an upland-GW-fen system within land surface models. The outcomes of this study can aid in improving process representation in LSMs and guiding current and future hydrological modelling practices in fen-dominated areas. However, other types of wetlands need more investigation using data/observations from different site conditions. This can result in more accurate simulation of the water cycle in those regions,

385   contributing to enhanced water resources management and allocation, as well as improving the LSMs' ability to predict the effects of future climate change on wetlands.

Data availability

We used the Water Information Systems KISTERS (WISKI) data. The data is publicly available on https://wiki.usask.ca/display/GWFDM/WISKI and were downloaded using the python WISKI tool (https://github.com/incsanchezro/WISKI_Tools_GWF). The meteorological data are from Old Jack Pine (OJP) and Fen flux towers, and the upland groundwater observations from OJP. The models developed and used in this paper are available at the following Zenodo repository https://doi.org/10.5281/zenodo.8277901.

Author contribution

ME: conceptualization, methodology, model development, writing; **AI**: conceptualization, methodology, model development and writing (review and edit); **SR**: conceptualization, methodology, writing (review and edit).

Competing interests

The authors declare that they have no conflict of interest.

Acknowledgements

We would like to thank the Global Water Futures (GWF) and the Integrated Modelling Program for Canada (IMPC) for funding this research.

References

Barr, A. G., van der Kamp, G., Black, T. A., McCaughey, J. H., and Nesic, Z.: Energy balance closure at the BERMS flux towers in relation to the water balance of the White Gull Creek watershed 1999–2009, Agricultural and Forest Meteorology, 153, 3–13, https://doi.org/10.1016/j.agrformet.2011.05.017, 2012.

Blyth, E. M., Arora, V. K., Clark, D. B., Dadson, S. J., De Kauwe, M. G., Lawrence, D. M., Melton, J. R., Pongratz, J., Turton, R. H., Yoshimura, K., and Yuan, H.: Advances in Land Surface Modelling, Curr Clim Change Rep, 7, 45–71, https://doi.org/10.1007/s40641-021-00171-5, 2021.

Canada Committee on Ecological (Biophysical) Land Classification (Ed.): Wetlands of Canada, Sustainable Development Branch, Canadian Wildlife Service, Conservation and Protection, Environment Canada, Ottawa, 452 pp., 1988.

Clark, M. P., Fan, Y., Lawrence, D. M., Adam, J. C., Bolster, D., Gochis, D. J., Hooper, R. P., Kumar, M., Leung, L. R., Mackay, D. S., Maxwell, R. M., Shen, C., Swenson, S. C., and Zeng, X.: Improving the representation of hydrologic processes

in Earth System Models: REPRESENTING HYDROLOGIC PROCESSES IN EARTH SYSTEM MODELS, Water Resour. Res., 51, 5929–5956, https://doi.org/10.1002/2015WR017096, 2015.

Dai, Y., Zeng, X., Dickinson, R. E., Baker, I., Bonan, G. B., Bosilovich, M. G., Denning, A. S., Dirmeyer, P. A., Houser, P.

415   R., Niu, G., Oleson, K. W., Schlosser, C. A., and Yang, Z.-L.: The Common Land Model, Bulletin of the American Meteorological Society, 84, 1013–1024, https://doi.org/10.1175/BAMS-84-8-1013, 2003.

Davison, B., Pietroniro, A., Fortin, V., Leconte, R., Mamo, M., and Yau, M. K.: What is Missing from the Prescription of Hydrology for Land Surface Schemes?, J. Hydrometeor, 17, 2013–2039, https://doi.org/10.1175/JHM-D-15-0172.1, 2016.

Fan, Y., Li, H., and Miguez-Macho, G.: Global Patterns of Groundwater Table Depth, Science, 339, 940–943,

420   https://doi.org/10.1126/science.1229881, 2013.

Fan, Y., Clark, M., Lawrence, D. M., Swenson, S., Band, L. E., Brantley, S. L., Brooks, P. D., Dietrich, W. E., Flores, A., Grant, G., Kirchner, J. W., Mackay, D. S., McDonnell, J. J., Milly, P. C. D., Sullivan, P. L., Tague, C., Ajami, H., Chaney, N., Hartmann, A., Hazenberg, P., McNamara, J., Pelletier, J., Perket, J., Rouholahnejad-Freund, E., Wagener, T., Zeng, X., Beighley, E., Buzan, J., Huang, M., Livneh, B., Mohanty, B. P., Nijssen, B., Safeeq, M., Shen, C., Verseveld, W., Volk, J.,

425   and Yamazaki, D.: Hillslope Hydrology in Global Change Research and Earth System Modeling, Water Resour. Res., 55, 1737–1772, https://doi.org/10.1029/2018WR023903, 2019.

Gingras, B., Slattery, S., Smith, K., and Darveau, M.: Boreal Wetlands of Canada and the United States of America, in: The Wetland Book: II: Distribution, Description, and Conservation, edited by: Finlayson, C. M., Milton, G. R., Prentice, R. C., and Davidson, N. C., Springer Netherlands, Dordrecht, 521–542, https://doi.org/10.1007/978-94-007-4001-3_9, 2018.

430   Goodbrand, A., Westbrook, C. J., and Kamp, G. van der: Hydrological functions of a peatland in a Boreal Plains catchment, Hydrological Processes, 33, 562–574, https://doi.org/10.1002/hyp.13343, 2019.

Goodbrand, A. R.: Influence of lakes and peatlands on groundwater contribution to boreal streamflow, MSc Thesis, University of Saskatchewan, 2013.

de Graaf, I. E. M., van Beek, R. L. P. H., Gleeson, T., Moosdorf, N., Schmitz, O., Sutanudjaja, E. H., and Bierkens, M. F. P.:

435   A global-scale two-layer transient groundwater model: Development and application to groundwater depletion, Advances in Water Resources, 102, 53–67, https://doi.org/10.1016/j.advwatres.2017.01.011, 2017.

Ireson, A. M., Sanchez-Rodriguez, I., Basnet, S., Brauner, H., Bobenic, T., Brannen, R., Elrashidy, M., Braaten, M., Amankwah, S. K., and Barr, A.: Using observed soil moisture to constrain the uncertainty of simulated hydrological fluxes, Hydrological Processes, 36, e14465, https://doi.org/10.1002/hyp.14465, 2022.

440   Kollet, S. J. and Maxwell, R. M.: Capturing the influence of groundwater dynamics on land surface processes using an integrated, distributed watershed model, Water Resources Research, 44, https://doi.org/10.1029/2007WR006004, 2008.

Larsen, M. a. D., Refsgaard, J. C., Drews, M., Butts, M. B., Jensen, K. H., Christensen, J. H., and Christensen, O. B.: Results from a full coupling of the HIRHAM regional climate model and the MIKE SHE hydrological model for a Danish catchment, Hydrology and Earth System Sciences, 18, 4733–4749, https://doi.org/10.5194/hess-18-4733-2014, 2014.

445   Letts, M. G., Roulet, N. T., Comer, N. T., Skarupa, M. R., and Verseghy, D. L.: Parametrization of peatland hydraulic properties for the Canadian land surface scheme, Atmosphere-Ocean, 38, 141–160, https://doi.org/10.1080/07055900.2000.9649643, 2000.

Manabe, S.: CLIMATE AND THE OCEAN CIRCULATION: I. THE ATMOSPHERIC CIRCULATION AND THE HYDROLOGY OF THE EARTH'S SURFACE, Monthly Weather Review, 97, 739–774, https://doi.org/10.1175/1520-

450   0493(1969)097<0739:CATOC>2.3.CO;2, 1969.

Maxwell, R. M. and Miller, N. L.: Development of a Coupled Land Surface and Groundwater Model, J. Hydrometeor., 6, 233–247, https://doi.org/10.1175/JHM422.1, 2005.

Maxwell, R. M., Chow, F. K., and Kollet, S. J.: The groundwater–land-surface–atmosphere connection: Soil moisture effects on the atmospheric boundary layer in fully-coupled simulations, Advances in Water Resources, 30, 2447–2466,

455   https://doi.org/10.1016/j.advwatres.2007.05.018, 2007.

Maxwell, R. M., Condon, L. E., and Kollet, S. J.: A high-resolution simulation of groundwater and surface water over most of the continental US with the integrated hydrologic model ParFlow v3, Geosci. Model Dev., 15, 2015.

Mitsch, W. J.: Wetlands of Canada: National Wetlands Working Group. Ecological Land Classification Series, 24. Sustainable Development Branch, Environment Canada, Ottawa, Ont. and Polyscience Publications, Inc., Montreal, Que., 1988.

460   Hardcover, 452 pp. ISBN 0-921317-13-1, Ecological Modelling, 53, 160–161, https://doi.org/10.1016/0304-3800(91)90152-Q, 1991.

Mitsch, W. J., Bernal, B., Nahlik, A. M., Mander, Ü., Zhang, L., Anderson, C. J., Jørgensen, S. E., and Brix, H.: Wetlands, carbon, and climate change, Landscape Ecol, 28, 583–597, https://doi.org/10.1007/s10980-012-9758-8, 2013.

Nazarbakhsh, M., Ireson, A. M., and Barr, A. G.: Controls on evapotranspiration from jack pine forests in the Boreal Plains

465   Ecozone, Hydrological Processes, 34, 927–940, https://doi.org/10.1002/hyp.13674, 2020.

Ogden, F. L.: Geohydrology: Hydrological Modeling, in: Encyclopedia of Geology (Second Edition), edited by: Alderton, D. and Elias, S. A., Academic Press, Oxford, 457–476, https://doi.org/10.1016/B978-0-08-102908-4.00115-6, 2021.

Pietroniro, A., Fortin, V., Kouwen, N., Neal, C., Turcotte, R., Davison, B., Verseghy, D., Soulis, E. D., Caldwell, R., Evora, N., and Pellerin, P.: Development of the MESH modelling system for hydrological ensemble forecasting of the Laurentian

470   Great Lakes at the regional scale, Hydrol. Earth Syst. Sci., 11, 1279–1294, https://doi.org/10.5194/hess-11-1279-2007, 2007.

Razavi, S. and Gupta, H. V.: A multi-method Generalized Global Sensitivity Matrix approach to accounting for the dynamical nature of earth and environmental systems models, Environmental Modelling & Software, 114, 1–11, https://doi.org/10.1016/j.envsoft.2018.12.002, 2019.

Razavi, S., Hannah, D. M., Elshorbagy, A., Kumar, S., Marshall, L., Solomatine, D. P., Dezfuli, A., Sadegh, M., and

475   Famiglietti, J.: Coevolution of machine learning and process-based modelling to revolutionize Earth and environmental sciences: A perspective, Hydrological Processes, 36, e14596, https://doi.org/10.1002/hyp.14596, 2022.

Rivera, A. (Ed.): Canada's groundwater resources, Fitzhenry & Whiteside, Markham, ON, 803 pp., 2014.

Canadian Digital Elevation Model, 1945-2011 - Open Government Portal: https://open.canada.ca/data/en/dataset/7f245e4d-76c2-4caa-951a-45d1d2051333, last access: 14 December 2022.

480 Scheidegger, J. M., Jackson, C. R., Muddu, S., Tomer, S. K., and Filgueira, R.: Integration of 2D Lateral Groundwater Flow into the Variable Infiltration Capacity (VIC) Model and Effects on Simulated Fluxes for Different Grid Resolutions and Aquifer Diffusivities, Water, 13, 663, https://doi.org/10.3390/w13050663, 2021.

Sridhar, V., Billah, M. M., and Hildreth, J. W.: Coupled Surface and Groundwater Hydrological Modeling in a Changing Climate, Groundwater, 56, 618–635, https://doi.org/10.1111/gwat.12610, 2018.

485 Virtanen, P., Gommers, R., Oliphant, T. E., Haberland, M., Reddy, T., Cournapeau, D., Burovski, E., Peterson, P., Weckesser, W., Bright, J., van der Walt, S. J., Brett, M., Wilson, J., Millman, K. J., Mayorov, N., Nelson, A. R. J., Jones, E., Kern, R., Larson, E., Carey, C. J., Polat, İ., Feng, Y., Moore, E. W., VanderPlas, J., Laxalde, D., Perktold, J., Cimrman, R., Henriksen, I., Quintero, E. A., Harris, C. R., Archibald, A. M., Ribeiro, A. H., Pedregosa, F., van Mulbregt, P., SciPy 1.0 Contributors, Vijaykumar, A., Bardelli, A. P., Rothberg, A., Hilboll, A., Kloeckner, A., Scopatz, A., Lee, A., Rokem, A., Woods, C. N.,

490 Fulton, C., Masson, C., Häggström, C., Fitzgerald, C., Nicholson, D. A., Hagen, D. R., Pasechnik, D. V., Olivetti, E., Martin, E., Wieser, E., Silva, F., Lenders, F., Wilhelm, F., Young, G., Price, G. A., Ingold, G.-L., Allen, G. E., Lee, G. R., Audren, H., Probst, I., Dietrich, J. P., Silterra, J., Webber, J. T., Slavič, J., Nothman, J., Buchner, J., Kulick, J., Schönberger, J. L., de Miranda Cardoso, J. V., Reimer, J., Harrington, J., Rodríguez, J. L. C., Nunez-Iglesias, J., Kuczynski, J., Tritz, K., Thoma, M., Newville, M., Kümmerer, M., Bolingbroke, M., Tartre, M., Pak, M., Smith, N. J., Nowaczyk, N., Shebanov, N., Pavlyk, O.,

495 Brodtkorb, P. A., Lee, P., McGibbon, R. T., Feldbauer, R., Lewis, S., Tygier, S., Sievert, S., Vigna, S., Peterson, S., More, S., et al.: SciPy 1.0: fundamental algorithms for scientific computing in Python, Nat Methods, 17, 261–272, https://doi.org/10.1038/s41592-019-0686-2, 2020.

Wheater, H. S., Pomeroy, J. W., Pietroniro, A., Davison, B., Elshamy, M., Yassin, F., Rokaya, P., Fayad, A., Tesemma, Z., Princz, D., Loukili, Y., DeBeer, C. M., Ireson, A. M., Razavi, S., Lindenschmidt, K.-E., Elshorbagy, A., MacDonald, M.,

500 Abdelhamed, M., Haghnegahdar, A., and Bahrami, A.: Advances in modelling large river basins in cold regions with Modélisation Environnementale Communautaire—Surface and Hydrology (MESH), the Canadian hydrological land surface scheme, Hydrological Processes, 36, e14557, https://doi.org/10.1002/hyp.14557, 2022.

Yalew, S. G., Pilz, T., Schweitzer, C., Liersch, S., van der Kwast, J., van Griensven, A., Mul, M. L., Dickens, C., and van der Zaag, P.: Coupling land-use change and hydrologic models for quantification of catchment ecosystem services, Environmental

505 Modelling & Software, 109, 315–328, https://doi.org/10.1016/j.envsoft.2018.08.029, 2018.

Zampieri, M., Serpetzoglou, E., Anagnostou, E. N., Nikolopoulos, E. I., and Papadopoulos, A.: Improving the representation of river–groundwater interactions in land surface modeling at the regional scale: Observational evidence and parameterization applied in the Community Land Model, Journal of Hydrology, 420–421, 72–86, https://doi.org/10.1016/j.jhydrol.2011.11.041, 2012.

510 Zeng, Y., Xie, Z., Liu, S., Xie, J., Jia, B., Qin, P., and Gao, J.: Global Land Surface Modeling Including Lateral Groundwater Flow, Journal of Advances in Modeling Earth Systems, 10, 1882–1900, https://doi.org/10.1029/2018MS001304, 2018.

Zhang, Z., Li, Y., Barlage, M., Chen, F., Miguez-Macho, G., Ireson, A., and Li, Z.: Modeling groundwater responses to climate change in the Prairie Pothole Region, Hydrology and Earth System Sciences, 24, 655–672, https://doi.org/10.5194/hess-24-655-2020, 2020.